

Standard energy function for grain boundary orientation fundamental zone

Author information

Wei Wan^{1, 2, *}

¹ *Institute for Advanced Study, Nanchang University, Nanchang 330031, China*

² *Institute of Photovoltaics, Nanchang University, Nanchang 330031, China*

* *Corresponding author, Email address: vanv@email.ncu.edu.cn*

Abstract

The success of grain boundary (GB) orientation fundamental zone (FZ) has connected GB structures across multiple crystallographic characters with their properties in a unique insight, but quantitative understandings of the structure-property relationship in the FZ are still lacking yet. Here, a theoretical derivation is proposed to transfer the well-known Read-Shockley relationship to the 3D FZ to form a standard energy function, which is **proven** to capture the simulated energy trends in a simple and accurate manner. The theorization therefore provides a basis for the establishment of modern GB energy functions.

Keywords: Grain boundary; Dislocation; Read-Shockley relationship

Numerous material properties are affected by grain boundaries (GBs) in polycrystalline materials [1–8]. Enhancement of the properties can be made by controlling the population and connectivity of different GB types [9–15], which is known as grain boundary engineering (GBE). GB properties depend on the five macroscopic characters, the misorientation (three) and the boundary-plane orientation (two), that characterize the GB structures. However, most GB characterization schemes would ignore the role of the GB plane orientation and instead focus just on the three misorientation characters, and sometimes simplify them to a single disorientation angle [16].

Focusing on a simplified description was due to both the size of the five-dimensional GB space [17, 18] and the cognition of simple $\Sigma 3^n$ GBs that take the majority of the real GB population [10, 15]. Also, it served the community so well to form the foundation of many classical frameworks of GB structure-property relationship, such as the Read-Shockley relationship [19, 20] that predicts GB structure and energy as a function of disorientation angle, the Frank-Bilby equation [21–24] that known as a bridge between microscopic and macroscopic degrees of freedom, the structural and polyhedral unit models [25–27] characterizing GB atomic structures, and the universality of GB phases among different materials with the same lattice [28, 29]. With the advent of advanced manufacturing technologies, it will soon be possible to precisely control several microstructural features including texture, GB character and triple junction network distributions [30, 31]. Therefore, the simplified description must be extended to capture the features of the 5D GB space, enabling full exploitation of both microstructure-sensitive synthesis and GBE in the material design.

Until now, noteworthy efforts towards understanding the complex GB structure-property relationship have been made [32–40]. Take the basic GB energy for an example, artificial empirical functions [41, 42]

were established for FCC and BCC metals to express the GB energy as a function of the full five characters. Revisions or variants of the classical Read-Shockley relationship were also proposed to capture the energies of low angle grain boundaries and further describe the general trends of GB energy [20, 40]. However, a notable obstacle in the establishment of reliable GB structure-property relationships in the 5D GB space is the lack of a standardized representation of GB plane orientations that naturally includes the crystallographic symmetry [43], although recent experimental and computational approaches facilitate the analysis of GB structures and properties in their full crystallographic details [29, 38, 44–46]. Fortunately, the GB plane orientation fundamental zone [47] that uniquely indexes a given GB crystallography is the inevitable tool towards that target.

This work aims to carry out a simple Read-Shockley formalism function that accurately captures the energies of low angle symmetric tilt, twist and mixed tilt-twist GBs in the fundamental zone. It also wishes to provide a good description of the energy trends of high angle GBs except for these deep cusps, by considering them as the overlap of dislocation cores. The validity of this function will be confirmed in comparison with the calculated low angle GB energies that span multiple macroscopic characters. It is started by writing the revised Read-Shockley relationship of Wan and Tang [40] as the following:

$$E_{\text{GB}}^{\text{mixed}}(\theta, \phi, \omega) = E_{\text{GB}}^{\text{tilt}}(\theta)[1 + k_1\omega] + E_{\text{GB}}^{\text{twist}}(\phi) + \theta\phi[E_c^{\text{loss}} - E_s^{\text{loss}} \ln(\theta\phi)][1 + k_2\omega] \quad (1)$$

Where θ is the tilt angle and ϕ is the twist angle of a decomposed low angle mixed GB. k_1 and k_2 are fitting parameters. The terms

$$E_{\text{GB}}^{\text{tilt}}(\theta) = \frac{\theta[E_c^{\text{tilt}} - E_s^{\text{tilt}} \ln(\theta)]}{|b^{\text{tilt}}|}, \quad (2)$$

$$E_{\text{GB}}^{\text{twist}}(\phi) = \frac{\phi[E_c^{\text{twist}} - E_s^{\text{twist}} \ln(\phi)]}{|b^{\text{twist}}|}$$

are the original Read-Shockley relationship for low angle symmetric tilt and twist GBs, respectively. Noting that the superscript tilt and twist denote the GB types, superscript c and s denote dislocation core and strain energy, respectively. E_c^{loss} and E_s^{loss} denote the losses of dislocation core energy and strain energy when a low angle mixed GB is formed by the energetically favorable dislocation glide and reaction mechanisms [40], respectively.

Writing the energy function of the 3D FZ in a polar coordinate manner:

$$E_{\text{GB}}^{\text{FZ}}(R, \psi, A) = \dots \quad (3)$$

Where R denotes the axial length of the polar coordinate and $0 \leq R \leq 1$. ψ denotes the rotation angle of the polar coordinate and $0 \leq \psi \leq \psi_{\text{symm}}$ (ψ_{symm} is defined by the symmetry. e.g., $\psi_{\text{symm}} = 45^\circ$ for [100] axis with D_{4h} symmetry). A denotes the GB misorientation angle in the R-F space and $0 \leq A \leq A_{\text{RF}}$ (A_{RF} is the constraint of the RF space). The schematic explanation of equation (3) is given in Figure 1.

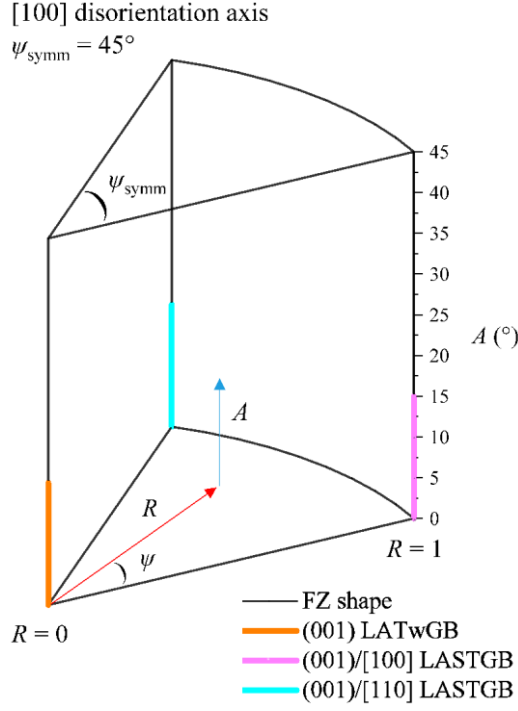


Figure 1. Illustration of the polar coordinate system to index a given GB with parameters R , ψ and A in the $[100]$ disorientation axis FZ.

Therefore, an arbitrary point P in the FZ is defined as $P(R\cos\psi, R\sin\psi, A)$ in a cartesian coordinate, and there must be:

$$\begin{aligned}
 E_{\text{GB}}^{\text{FZ}}(0, 0, A) &= \frac{A \left[E_c^{\text{twist}} - E_s^{\text{twist}} \ln(A) \right]}{|b^{\text{twist}}|} = E_{\text{GB}}^{\text{twist}}(A), \\
 E_{\text{GB}}^{\text{FZ}}(1, 0, A) &= \frac{A \left[E_c^{\text{tilt}} - E_s^{\text{tilt}} \ln(A) \right]}{|b^{\text{tilt}}|} = E_{\text{GB}}^{\text{tilt}}(A), \\
 E_{\text{GB}}^{\text{FZ}}(1, \psi_{\text{symm}}, A) &= \frac{A \left[E_c^{\text{tilt}} - E_s^{\text{tilt}} \ln(A) \right]}{|b^{\text{tilt}}|} \left[1 + k_1 \psi_{\text{symm}} \right] = E_{\text{GB}}^{\text{tilt}}(\theta) \left[1 + k_1 \psi_{\text{symm}} \right]
 \end{aligned} \tag{4}$$

Where $R = 0$ yields LATwGB in FZ and $R = 1$ yields LASTGB in FZ. Thus, for any axial lines that have a given ψ and A values, a smooth transition from LATwGB to LASTGB must be observed. Therefore, we can write R as the following:

$$R = TTR = \frac{\theta}{\theta + \phi} \tag{5}$$

Parameter TTR , known as the tilt-twist ratio, defines the topology of LAMGB and $TTR = 0$ yields LATwGB in the mixed character space and $TTR = 1$ yields LASTGB in the mixed character space (<https://arxiv.org/abs/2403.02070>). In so doing, the physical meanings of TTR have been translated to 3D FZ. Meanwhile, A could be written following the methods of Wan and Tang:

$$A = \sqrt{\theta^2 + \phi^2} \tag{6}$$

Hence, the energy function in a 2D plane (R, A) of the 3D FZ is given as a function of R and A following

$$E_{\text{GB}}^{\text{FZ}}(R, A) = \frac{A \left[E_{\text{c}}^{\text{twist}} - E_{\text{s}}^{\text{twist}} \ln(A) \right]}{|b^{\text{twist}}|} (1-R) + \frac{A \left[E_{\text{c}}^{\text{tilt}} - E_{\text{s}}^{\text{tilt}} \ln(A) \right]}{|b^{\text{tilt}}|} R + R(1-R) \left[E_{\text{c}}^{\text{loss}} - E_{\text{s}}^{\text{loss}} \ln(R(1-R)) \right] \quad (7)$$

We then consider the role of ψ . Assuming that GB energy varies smoothly (ignore the Read-Shockley peaks) in the low angle part ($0^\circ \leq A \leq 15^\circ$) of the 3D FZ, and using a linear interpolation between $E_{\text{GB}}^{\text{FZ}}(1, 0, A)$ and $E_{\text{GB}}^{\text{FZ}}(1, \psi_{\text{symm}}, A)$ yields

$$E_{\text{GB}}^{\text{FZ}}(R, \psi, A) = \frac{A \left[E_{\text{c}}^{\text{twist}} - E_{\text{s}}^{\text{twist}} \ln(A) \right]}{|b^{\text{twist}}|} (1-R) [1 + k_1 \psi] + \frac{A \left[E_{\text{c}}^{\text{tilt}} - E_{\text{s}}^{\text{tilt}} \ln(A) \right]}{|b^{\text{tilt}}|} R + R(1-R) \left[E_{\text{c}}^{\text{loss}} - E_{\text{s}}^{\text{loss}} \ln(R(1-R)) \right] [1 + k_2 \psi] \quad (8)$$

A worse case is that the dislocation core and strain energies of the original Read-Shockley relationship are not linearly correlated at $E_{\text{GB}}^{\text{FZ}}(1, 0, A)$ and $E_{\text{GB}}^{\text{FZ}}(1, \psi_{\text{symm}}, A)$ and the total energy is linearly correlated, which then yields:

$$E_{\text{GB}}^{\text{FZ}}(R, \psi, A) = \frac{A \left[E_{\text{c}}^{\text{twist}} - E_{\text{s}}^{\text{twist}} \ln(A) \right]}{|b^{\text{twist}}|} (1-R) + \frac{A \left[E_{\text{c}, \psi=0}^{\text{tilt}} - E_{\text{s}, \psi=0}^{\text{tilt}} \ln(A) \right]}{|b^{\text{tilt}}|} R + \frac{A \left[\left(E_{\text{c}, \psi=\psi_{\text{symm}}}^{\text{tilt}} - E_{\text{s}, \psi=0}^{\text{tilt}} \right) - \left(E_{\text{s}, \psi=\psi_{\text{symm}}}^{\text{tilt}} - E_{\text{s}, \psi=0}^{\text{tilt}} \right) \ln(A) \right]}{|b^{\text{tilt}}|} R \frac{\psi}{\psi_{\text{symm}}} + R(1-R) \left[E_{\text{c}}^{\text{loss}} - E_{\text{s}}^{\text{loss}} \ln(R(1-R)) \right] [1 + k_2 \psi] \quad (9)$$

Where $E_{\text{c}, \psi=0}^{\text{tilt}}$, $E_{\text{s}, \psi=0}^{\text{tilt}}$, $E_{\text{c}, \psi=\psi_{\text{symm}}}^{\text{tilt}}$ and $E_{\text{s}, \psi=\psi_{\text{symm}}}^{\text{tilt}}$ are the dislocation core and strain energies of LASTGBs at $\psi = 0$ and $\psi = \psi_{\text{symm}}$, respectively. Note that one must at least know the energy of six points on the FZ surface to further interpolate the energy trend inside under the framework of equations (8) or (9). Three of the six points are located on the three vertices of a given 2D FZ and the others are located on the three sides of the 2D FZ but no limitations to their values of A .

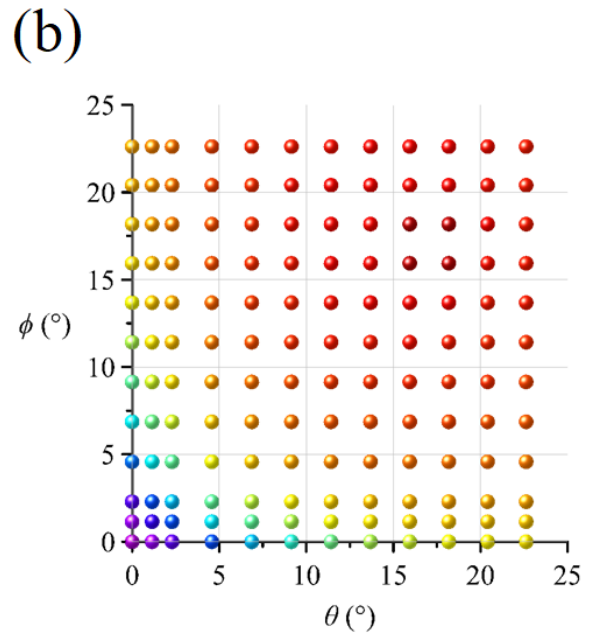
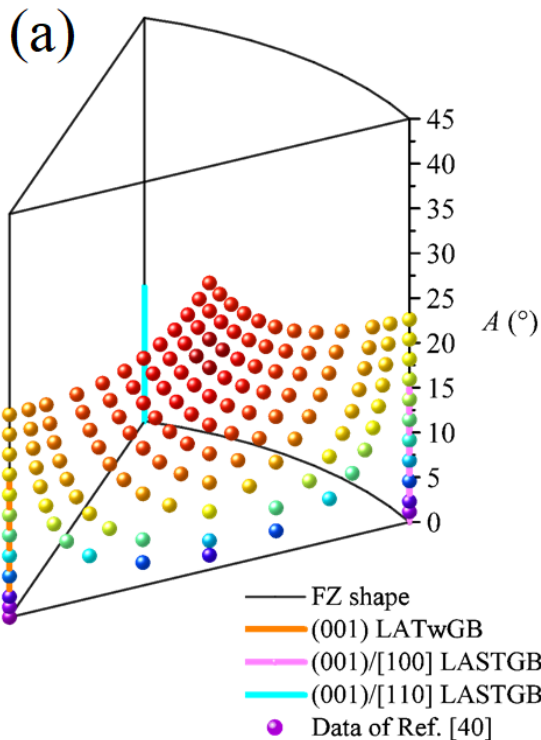


Figure 2. (a) Mapping the data of Wan and Tang [40] to the fundamental zone; (b) Energies of 121 (001)/[100] low angle mixed grain boundaries as a function of tilt angle θ and twist angle ϕ [40]. The energy data shown in Figure 2b is used with permission.

Figure 2a shows the energies of silicon (001)/[100] low angle mixed GBs as a function of R and A . The figure is plotted by converting the conventional tilt and twist angular description of the low angle mixed GBs to the 3D FZ description. It can be seen that the theoretical derivation correctly converted the parameter TTR of low angle mixed GBs to FZ parameter R .

In this short letter, the analytical expressions of the original Read-Shockley relationship and its advanced form have been defined in the FZ as a function of three FZ parameters, which would be useful to interpolate the energy trends within the low angle part of the FZ. **The theoretical derivation is subjected to the comparison with simulation to further confirm its validity.** Since high angle GBs are usually considered as the overlap of dislocation cores, the energy trends of LAGBs somehow provide a brief preview of the energy trends spanning the entire FZ. Benefited from the advantages of uniquely characterizing the GBs, the Read-Shockley functional form defined in the FZ has a better performance than the original Read-Shockley relationship (and its variants), and such functional form is expected to be a starting point for any modern GB energy functions that are artificially built for predicting the energy cusps in the 5D GB space.

Data availability

Numerical data are NOT involved in this theoretical study.

Acknowledgements

W. Wan acknowledges the insightful discussions with Prof. E.R. Homer from Brigham Young University. The manuscript is written in a single day.

Competing interests

The author declares no competing interests.

Fundings

This work received NO financial support.

Author contributions

There is only one author.

References

- [1] Hall, E.O. The Deformation and Ageing of Mild Steel: III Discussion of Results. *Proc. Phys. Soc. B* **1951**, 64, 747–753.
- [2] Petch, N.J. The Cleavage Strength of Polycrystals. *J. Iron Steel Inst.* **1953**, 174, 25–28.
- [3] Hansen, N. Hall–Petch relation and boundary strengthening. *Scripta Mater.* **2004**, 51, 801–806.
- [4] Chiba, A.; Hanada, S.; Watanabe, S.; Abe, T.; Obana, T. Relation Between Ductility and Grain-Boundary Character Distributions in Ni₃Al. *Acta Metall. Mater.* **1994**, 42, 1733–1738.
- [5] Shimada, M.; Kokawa, H.; Wang, Z.J.; Sato, Y.S.; Karibe, I. Optimization of grain boundary character distribution for

- intergranular corrosion resistant 304 stainless steel by twin-induced grain boundary engineering. *Acta Mater.* **2002**, *50*, 2331–2341.
- [6] Lu, L. Ultrahigh Strength and High Electrical Conductivity in Copper. *Science* **2004**, *304*, 422–426.
- [7] Bagri, A.; Kim, S.P.; Ruoff, R.S.; Shenoy, V.B. Thermal transport across Twin Grain Boundaries in Polycrystalline Graphene from Nonequilibrium Molecular Dynamics Simulations. *Nano Lett.* **2011**, *11*, 3917–3921.
- [8] Meyers, M.A.; Mishra, A.; Benson, D.J. Mechanical properties of nanocrystalline materials. *Prog. Mat. Sci.* **2006**, *51*, 427–556.
- [9] Watanabe, T. An approach to grain boundary design for strong and ductile polycrystals. *Res. Mech.* **1984**, *11*, 47.
- [10] Randle, V. Grain boundary engineering: an overview after 25 years. *Mater. Sci. Tech.-Lond.* **2010**, *26*, 253–261.
- [11] Randle, V.; Jones, R. Grain boundary plane distributions and single-step versus multiple-step grain boundary engineering. *Mater. Sci. Eng. A* **2009**, *524*, 134–142.
- [12] Schlegel, S.M.; Hopkins, S.; Frary, M. Effect of grain boundary engineering on microstructural stability during annealing. *Scripta Mater.* **2009**, *61*, 88–91.
- [13] Randle, V.; Coleman, M. A study of low-strain and medium-strain grain boundary engineering. *Acta Mater.* **2009**, *57*, 3410–3421.
- [14] Engelberg, D.L.; Newman, R.C.; Marrow, T. J. Effect of thermomechanical process history on grain boundary control in an austenitic stainless steel. *Scripta Mater.* **2008**, *59*, 554–557.
- [15] Palumbo, G.; Lehockey, E.; Lin, P. Applications for grain boundary engineered materials. *JOM* **1998**, *50*, 40–43.
- [16] Rohrer, G.S. Grain boundary energy anisotropy: a review. *J. Mater. Sci.* **2011**, *46*(18), 5881–5895.
- [17] Patala, S.; Mason, J. K.; Schuh, C. A. Improved representations of misorientation information for grain boundary science and engineering. *Prog. Mater. Sci.* **2012**, *57*, 1383–1425.
- [18] *Materials Interfaces: Atomic-level structure and properties* (eds Wolf, D. & Yip, S.), (Chapman & Hall, 1992)
- [19] Read, W.T.; Shockley, W. Dislocation models of crystal grain boundaries. *Phys. Rev.* **1950**, *78*(3), 275–289.
- [20] Wolf, D. A Read-Shockley model for high-angle grain boundaries, *Scr. Metall.* **1989**, *23*(10), 1713–1718.
- [21] Frank, F.C. Conference on plastic deformation of crystalline solids. Carnegie Institute of Technology and Office of Naval Research. **1950**, 150.
- [22] Bilby, B.A. Continuous distribution of dislocations. *Prog. Solid. Mech.* **1960**, *1*, 329.
- [23] Yang, J.B.; Nagai, Y.; Hasegawa, M. Use of the Frank–Bilby equation for calculating misfit dislocation arrays in interfaces. *Scr. Mater.* **2010**, *62*(7), 458–461.
- [24] Yang, J.B.; Nagai, Y.; Yang, Z.G.; Hasegawa, M. Quantization of the Frank–Bilby equation for misfit dislocation arrays in interfaces. *Acta Mater.* **2009**, *57*, 4874–4881.
- [25] Sutton, A.P. On the structural unit model of grain boundary structure. *Philos. Mag. Lett.* **1989**, *59*(2), 53–59.
- [26] Han, J.; Vitek, V.; Srolovitz, D.J. The grain-boundary structural unit model redux. *Acta Mater.* **2017**, *133*, 186–199.
- [27] Banadaki, A.D.; Patala, S. A three-dimensional polyhedral unit model for grain boundary structure in fcc metals. *npj Comput. Mater.* **2017**, *3*(1), 13.
- [28] Brink, T.; Langenohl, L.; Bishara, H.; Dehm, G. Universality of grain boundary phases in fcc metals: Case study on high-angle [111] symmetric tilt grain boundaries. *Phys. Rev. B* **2023**, *107*(5), 054103.
- [29] Meiners, T.; Frolov, T.; Rudd, R.E.; Dehm, G.; Liebscher, C.H. Observations of grain-boundary phase transformations in an elemental metal. *Nature* **2020**, *579*(7799), 375–378.
- [30] Dehoff, R.R.; Kirka, M.M.; Sames, W.J.; Bilheux, H.; Tremsin, A.S.; Lowe, L.E.; Babu, S.S. Site specific control of crystallographic grain orientation through electron beam additive manufacturing. *Mater. Sci. Tech.-Lond.* **2015**, *31*, 931–938.
- [31] Johnson, O.K.; Schuh, C.A. The uncorrelated triple junction distribution function: Towards grain boundary network design. *Acta Mater.* **2013**, *61*, 2863–2873.
- [32] Olmsted, D.L.; Foiles, S.M.; Holm, E.A. Survey of computed grain boundary properties in face-centered cubic metals: I. Grain boundary energy. *Acta Mater.* **2009**, *57*, 3694.
- [33] Homer, E.R. High-throughput simulations for insight into grain boundary structure-property relationships and other

- complex microstructural phenomena. *Comput. Mater. Sci.* **2019**, 161, 244–254.
- [34] Homer, E.R.; Holm, E.A.; Foiles, S.M.; Olmsted, D.L. Trends in Grain Boundary Mobility: Survey of Motion Mechanisms. *JOM* **2014**, 66(1), 114–120.
- [35] Von Alfthan, S.; Haynes, P.D.; Kaski, K.; Sutton, A.P. Are the structures of twist grain boundaries in silicon ordered at 0K. *Phys. Rev. Lett.* **2006**, 96, 055505.
- [36] Sharp, T.A.; Thomas, S.L.; Cubuk, E.D.; Schoenholz, S.S.; Srolovitz, D.J.; Liu, A.J. Machine learning determination of atomic dynamics at grain boundaries. *Proc. Natl. Acad. Sci.* **2018**, 115(43), 10943–10947.
- [37] Erickson, H.C.; Homer, E.R. Insights into grain boundary energy structure-property relationships by examining computed [1 0 0] disorientation axis grain boundaries in Nickel. *Scr. Mater.* **2020**, 185, 165–169.
- [38] Homer, E.R.; Hart, G.L.W.; Owens, C.B.; Hensley, D.M.; Spendlove, J.C.; Serafinb, L.H. Examination of computed aluminium grain boundary structures and energies that span the 5D space of crystallographic character. *Acta Mater.* **2022**, 234, 118006.
- [39] Wan, W.; Tang, C.X.; Zou, W.N. Exploring Silicon [001] Small Angle Symmetric Tilt Grain Boundaries: Structures, Energies and Stress fields. *Applied Surface Science* **2022**, 599, 153828.
- [40] Wan, W.; Tang, C.X. Structures and energies of computed silicon (001) small angle mixed grain boundaries as a function of three macroscopic characters. *Acta Mater.* **2023**, 261, 119353.
- [41] Bulatov, V.V.; Reed, B.W.; Kumar, M. Grain boundary energy function for fcc metals. *Acta Mater.* **2014**, 65, 161–175.
- [42] Chirayutthanasak, O.; Sarochawikasit, R.; Khongpia, S.; Okita, T.; Dangtip, S.; Rohrer, G.S.; Ratanaphan, S. Universal function for grain boundary energies in bcc metals. *Scr. Mater.* **2024**, 240, 115821.
- [43] Patala, S.; Schuh, C.A. Symmetries in the representation of grain boundary plane distributions. *Philos. Mag.* **2013**, 93(5), 524–573.
- [44] Yu, Z.Y.; Cantwell, P.R.; Gao, Q.; Yin, D.; Zhang, Y.Y.; Zhou, N.X.; Rohrer, G.S.; Widom, M.; Luo, J.; Harmer, M.P. Segregation-induced ordered superstructures at general grain boundaries in a nickel-bismuth alloy. *Science* **2017**, 358, 97–101.
- [45] Akatsu, T.; Scholz, R.; Gosele, U. Dislocation structure in low-angle interfaces between bonded Si(001) wafers. *J. Mater. Sci.* **2004**, 39(9), 3031–3039.
- [46] Zhu, Q.; Samanta, A.; Li, B.; Rudd, R.E.; Frolov, T. Predicting phase behavior of grain boundaries with evolutionary search and machine learning. *Nat. Commun.* **2018**, 9(1), 467.
- [47] Homer, E.R.; Patala, S.; Priedeman, J.L. Grain boundary plane orientation fundamental zones and structure-property relationships. *Sci. Rep.* **2015**, 5, 15476.